Available online at www.sciencedirect.com

ScienceDirect

Transportation Research Procedia 14 (2016) 2006 – 2014

Transportation Research Procedia

www.elsevier.com/locate/procedia

6th Transport Research Arena April 18-21, 2016

Fracture mechanics based approach to the significance of certain loads on the service life of rails

Senta Pessel [a,*], Martin Mensinger [a]

[a]*Technical University of Munich, Arcisstr. 21, 80333 München, Germany*

Abstract

In this paper, the fatigue design of rails in the transition from bridge to abutment is examined. The current fatigue design of rail systems is carried out with simplifying assumptions concerning the stresses in the rail. Thus, the determination of a fatigue endurance limit is done with stresses based on the Smith-Diagram. By applying this means of design, the assumption is made that there are mainly normal stresses in a rail. Those may originate from changes in temperature, accelerating or slowing down of the trains as well as bending stresses caused by the passing of trains. Horizontal components of the load (from the train's sine run, lateral shift of bridges or the cant of curves) are not considered in this design format.

At the same time, specimens in fatigue tests with pulsing vertical loads regularly show unexpected and inexplicable cracks at the edge of the rail foot and a huge scatter of the results. In cases of rail breaks the location of the incipient crack is not necessarily in the cross section's area with the largest tensile stresses, but can be shifted to areas of smaller tensile stress (e.g. the edge of the rail foot).

Obviously additional criteria such as the condition of the surface of the rail foot in combination with stresses from warping of the section (secondary bending) have more influence on the fatigue performance than estimated before.

This paper presents an approach to evaluate the importance and priorities of the named influencing factors and criteria on the fatigue design of rails by means of fracture mechanics. The focus hereby lies on the rail foot, since in this region of the cross section there are no disturbing influences as contact problems or wear.

© 2016 The Authors. Published by Elsevier B.V. This is an open access article under the CC BY-NC-ND license (http://creativecommons.org/licenses/by-nc-nd/4.0/).

Peer-review under responsibility of Road and Bridge Research Institute (IBDiM)

* Corresponding author. Tel.: +49-89-289-22525; fax: +49-89-289-22522.
E-mail address: senta.pessel@tum.de

2352-1465 © 2016 The Authors. Published by Elsevier B.V. This is an open access article under the CC BY-NC-ND license (http://creativecommons.org/licenses/by-nc-nd/4.0/).
Peer-review under responsibility of Road and Bridge Research Institute (IBDiM)
doi:10.1016/j.trpro.2016.05.168

Keywords: lateral displacement; fracture mechanics; rail foot

1. Introduction

This paper is based on the investigations of an AiF FOSTA research project, which has been granted in 2014. Participants of the project are the Chair of Metal Structures, the Chair of Concrete Structures and the Chair of Road, Railway and Airfield Construction at the Technical University of Munich.

The aim of the project is to have a closer look at the fatigue of continuously welded railway rails subjected to horizontal loads. In the current fatigue design, which is carried out using the EN 1991-2, only normal and bending stresses are considered in the design process. But in regions of curves or in the transition from abutment to bridge horizontal forces lead to warping and bending around the weak axle of the cross-section. In order to find out more about the importance of these additional stresses in the project fracture mechanical approaches are used in order to evaluate the importance of these horizontal loads.

In this paper, first of all the current design concept is described. The influences which are taken into account at the moment and those who have been ignored so far are pointed out. As all of the current concepts are to be found in the field of fatigue design, it will be described how the transition to fracture mechanical problems can be made and how these concepts can lead to an extension of the current design concepts in order to take into account horizontal loads.

2. The current design concept

In Germany railroad rails are designed to be fatigue resistant. Consequently, the loads they have to bear are so small that they can be applied “as often as one likes” during the life cycle (Haibach (2006)). Edel (2015) states from his own experience that if a bearing member made from steel does not fail after $2 \cdot 10^6$ load cycles of testing it may be considered as fatigue resistant on the stress-level tested.

The before mentioned fatigue tests are also known as Wöhler fatigue tests. According to Kopp (1970), for every number of stress cycles N a corresponding fatigue strength σ_{Schw} can be determined. In the fatigue strength diagram of Smith a link between this fatigue strength and the admissible loads can be found. Kopp (1970) declares that for differing minimum stresses σ_{U} the corresponding live loads σ_Q can be determined with this diagram.

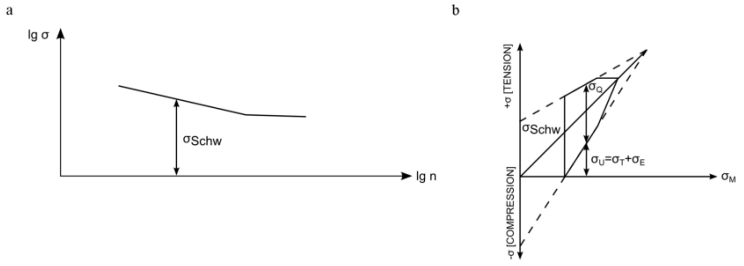

Fig. 1. (a) Wöhler curve and (b) Smith diagram according to Kopp (1970).

In Freystein (2012) an example is shown that illustrates these procedures for the design of rails in the track superstructure (figure 2). The example originally was published in Deutsche Bahn (1989). In figure 2 different processes are included. The first is the derivation of the Smith-Diagram. Taking into account the material’s tensile strength of $\sigma_{\mathrm{B}} = 900$ MPa, the yield strength of $\sigma_{0.2} = 470$ MPa and the testing results found on corroded railway rails by the chair of Road, Railway and Airfield Construction at Technische Universität München stating that $\sigma_{\mathrm{Schw}} = 205$ MPa ($\sigma_{\mathrm{U}} = 50$ MPa), the Smith-Diagram can be drawn. In the presented case the residual stresses $\sigma_{\mathrm{E}} = 80$ MPa and the stresses resulting from a temperature change of 50 K ($\sigma_{\mathrm{T}} = 120$ MPa) can also be found in

the diagram. Now the live loads σ_Q= 158 MPa have to be fitted in the diagram leading to the permitted bending strength for fatigue zulσ_{bD} = 160 MPa. Summing up these stresses a total stress of 358 MPa is the outcome. This leaves a free stress contingent of σ_{free} = 112 MPa that the rail can bear before reaching its fatigue limit in the given constellation. After subtracting 20 MPa for tensile stresses from the bending of the bridges under a passing train, a contingent of 92 MPa is left which can be distributed on stresses from rotation and displacement of the bridge's end, thermal expansion of the bridge, starting and breaking of the trains.

In the suitable code (EN 1991-2 (2012)) it is only stated, that for rails with tensile strength of at least 900 MPa in straight tracks or wide curves on macadam superstructure a free tensile stress contingent of 92 MPa is available and shall not be exceeded.

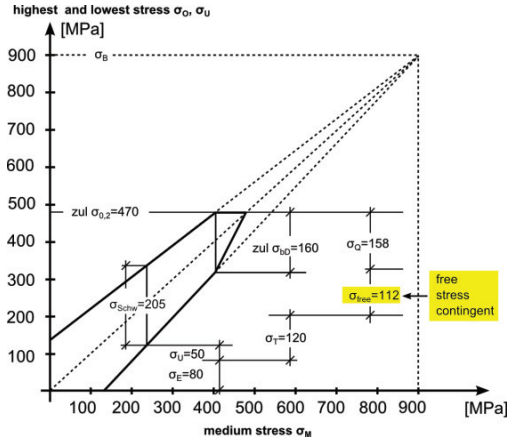

Fig. 2. Stress shares in the rail foot (60 E2, 900 N/mm²) from Freystein (2012).

As stated before, all the considerations mentioned above only apply to bending stresses resulting from vertical loads and normal stresses in the rail. The horizontal loads affecting the rails are not taken into account. During the last few years this has led to a lot of confusion amongst engineers because some bridges in the course of new high--speed railway tracks show larger horizontal movements than their older predecessors. The question arose if and how these lateral loads shall be included in the loads that have to be covered by the free tensile stress contingent.

3. Horizontal loads

As stated in section 2, horizontal loads aren't yet included in the fatigue design of railway rails. Mainly the stresses resulting from the so called "lateral displacement" are missing in the calculation schemes. The term lateral displacement describes the displacement of the end of the bridge deck compared to the abutment orthogonal to the rails (see also figure 3 for an illustration). As a consequence of these displacements the rail is loaded by additional transverse bending and warping. This leads to additional stresses in the rail foot (Schramm (2014)). It is a main question of research, how these stresses shall be superposed with stresses from other loads. Ruge at al. (2005) show that a simple superposition of loads on bridges leads to conservative results (resulting in larger stresses than in reality). Therefore attention has to be paid to how the loads are superposed and which loads are present in specific mounting locations (see also figure 4).

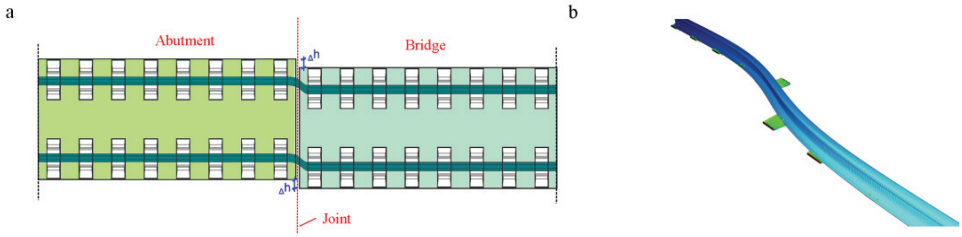

Fig. 3. Schematic representation of the lateral displacement Δh by Schramm (2014).

Load component		Location		
		Straight track	Curve	Transition bridge – abutment
Train	Vertical load	X	X	X
	Skew track		X	X
	Sine run and eccentric load	X	X	X
	Acceleration / breaking	X	X	X
Temperature	Solar radiation	X	X	X
	Convection	X	X	X
Building	Thermal expansion			X
	Lateral displacement			X
	Rotation			X
Substructure		X	X	X
Rail clamp		X	X	X
Residual stresses of the rail		X	X	X

Fig. 4. Combination of the relevant load components for stresses in the rail foot.

4. Application of fracture mechanics

At this point it seems self-evident to conduct more Wöhler fatigue tests with different combinations of vertical and horizontal loads in order to find out if the free stress contingent should be reduced in presence of horizontal loads, or not. Unfortunately, even the standardized fatigue tests that include only vertical loads show unexpected failure patterns. For example four-point-bending Wöhler tests didn't only show cracks from the middle of the rail foot (where the largest bending stresses can be found) but also from the corner of the upper part of the rail foot (see also figure 5). Considering these pictures it can be concluded that not only the loads play an important role in the fatigue crack initiation and failure of the rail. Therefore, fracture mechanics were chosen as the means to describe the influences on the cracks. Afterwards, conclusions may be drawn on the fatigue behaviour of the rails.

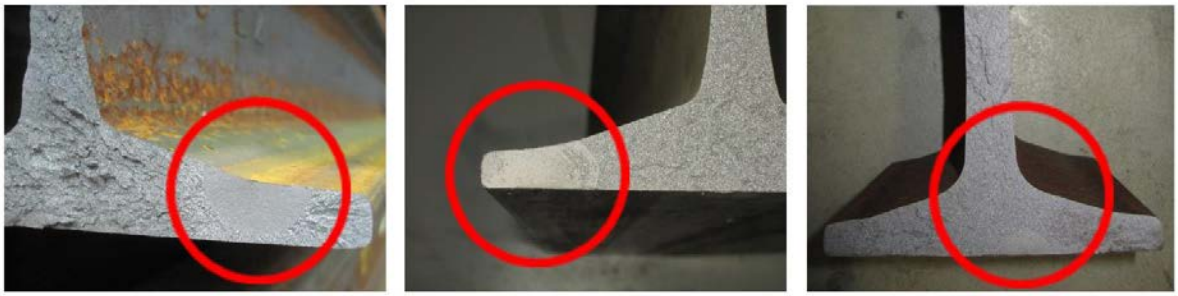

Fig. 5. Different crack locations after Wöhler tests.

Fracture mechanical methods are based on the assumption that a crack is present. For this crack it can be calculated if the crack is large enough to grow under certain loads and also how long it will take until the crack leads to the failure of the specimen. The easiest and most commonly used formula to describe the crack growth is the PARIS-law:

$$\frac{da}{dN} = C \cdot (\Delta K)^n \tag{1}$$

In this formula *da/dN* describes the crack growth *a* after a certain amount of load cycles *N*. *n* (often also called *m*) is a material dependent exponent. *C* depends on the load ratio *R* and on the material. As *C* and *n* are determined from the same experiments they are linked (see also Table 1). ΔK describes the stress intensity at the crack tip. This factor depends on the geometry of the probe, of the loads applied and on the depth of the crack. The crack growth rate *da/dN* can be written as a function of different parameters (Deutscher Stahlbau-Verband (1996)):

$$\frac{da}{dN} = f(\Delta K, R, T, Load, Material, Geometry, \dots) \tag{2}$$

Via Integration of the PARIS-law, the service life of a given probe can be calculated. The limits of this integration are given by the geometry, the fracture toughness K_{th} and the maximal stress intensity factor K_{IC}.

Thus it can be shown via simulations if a given load series can lead to crack growth and even component failure, or not. Figure 4 already shows that a lot of influences have to be taken into consideration in order to conduct meaningful simulations. But the outcome of fracture mechanical simulations does not only depend on the stresses that are inserted into the calculations. Most of the material properties aren't independent as well. Figure 6 illustrates this fact. As an example it can be seen which influences and resistances are dependent from a change of temperature. This poses huge challenges when for example an analysis of the total service lives *N* (calculated with the variables shown in figure 6) is to be conducted. Then *N* could be considered as the dependent variable that is calculated from a choice of independent variables. Unfortunately, figure 6 illustrates that most of the independent variables aren't independent. Those interdependencies pose a lot of problems in statistics. Therefore, a less complex example is studied in section 5 in order to get a first insight in the mechanisms.

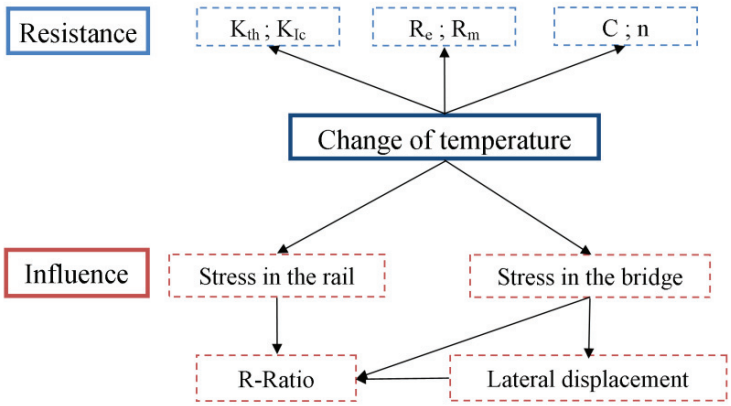

Fig. 6. Dependencies of variables.

5. Example: SENB3-specimens

Before the whole lifetime of fracture mechanical rail specimens with varying loads is simulated, approaches to determine the significance of given influences have to be developed. In this paper therefore the failure of a three--point-bending specimen (SENB3) according to BSI 12108 (2012) is studied.

Assuming that specimen like the one displayed in figure 7 shall be extracted from the rail foot, because of the geometry of the rail foot and the regulations of the standard, only certain ranges of parameters are valid. Now it is to be determined if there are parameters where small changes of the parameter cause a huge change in the achieved service life *N*. On the other hand, there might be parameters that change considerably and that don't really affect *N*. The simulated experiments are conducted like K-increasing-tests. This means that the load is kept constant even if the crack is growing.

The K-factor is calculated using the following two formulae where $\alpha = a/W$ with $0 \leq \alpha \leq 1.0$:

$$K = \frac{F}{BW^{1/2}} g\left(\frac{a}{W}\right) \tag{3}$$

$$g\left(\frac{a}{W}\right) = \frac{6\alpha^{1/2}}{[(1+2\alpha)(1-\alpha)^{3/2}]}[1.99 - \alpha(1-\alpha)(2.15 - 3.93\alpha + 2.7\alpha^2)] \tag{4}$$

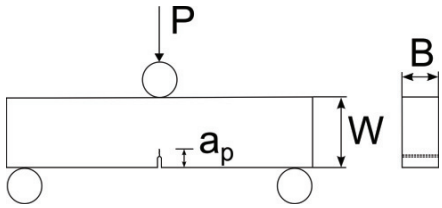

Fig. 7. SENB3 specimen according to BSI 12108:2012.

As variable parameters the specimen height *W*, the precrack length a_p (consisting of the cut notch and the fatigue precrack) and the load *P* have been chosen. The PARIS-parameters *C* and *n* are also varied. They depend on the load ratio *R* and the temperature *T* of the test environment. Thus *R* and *T* could be varied indirectly by varying the PARIS-parameters. In the following calculations data for *C* and *n* at +20 °C and R=0.1 have been chosen. In figure 8 the dependencies of the variables are shown.

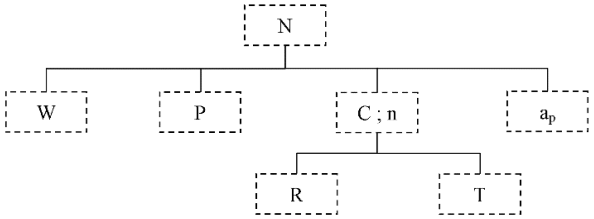

Fig. 8. Parameters.

In this paper, only six combinations of these parameters are presented. In table 1 the different combinations of the parameters are given. The first entry is referred to as the standard combination. For the other rows only the varied parameter is given.

For the values of *C* and *n* the fact has to be considered, that the values taken from Tóth (1980) are quite old and that the original literature could not be accessed by the authors. Therefore the results have to be handled with care, as there have been huge advances in steel technology since then. In the FOSTA project presented here these values will be measured in recently produced rails (see also section 6).

Table 1. Parameter combinations for the calculations.

Name	ap [mm]	W [mm]	P [N]	$C\ [\frac{mm}{cycle}\left(\frac{N}{mm^{3/2}}\right)^{-n}]$	*n*	Reference for *C* and n	Originally published in
Standard	3	22	3500	$1.8126 \cdot 10^{-18}$	4.77	Edel 2015	Schnitzer 2014
Var1_n=2.67				$7.48 \cdot 10^{-13}$	2.67	Edel 2015	Tóth 1980
Var2_n=2.81				$4.23 \cdot 10^{-13}$	2.81	Edel 2015	Tóth 1980
Var3_P=4500			4500				
Var4_ap=2.2	2.2						
Var5_W=25		25					

As a first attempt to get some insight into the calculations, the graphs given in figure 9 are made. Figure 9a) represents an *a-N*-plot of the cracks calculated. It can be observed, that Var4_ap2.2 starts at a lower value of a which was intended by the variation of a_p. It can also be seen, that the calculations don't end at the same value of a. This is caused by the calculation algorithm which stops the calculations either at $a = 0.6 \cdot W$ or at $\Delta K > K_{IC}$. In all examples the abortion of the calculation is related to the maximal stress intensity factor of $K_{IC} = 948\ N/mm^{3/2}$ (derived from Romano et al. (2015)) that was reached by the calculation and thus lead to abortion. In general it can be observed, that larger specimens and smaller starter cracks lead to a longer lifetime of the probes. In contrast to that observation, larger loads lead to a reduced lifetime.

In figure 9b) a log-log plot of *da/dN*-ΔK can be found. This plot can be interpreted as the speed of crack growth *da/dN* at a given stress intensity at the crack tip. In a log-log-plot these graphs appear as straight lines. It can easily be seen that only the variation in *C* and *n* causes differences in the graphs. The variations in the probe geometry and the loads can only be observed in the beginning of the graph with standard *C* and *n*.

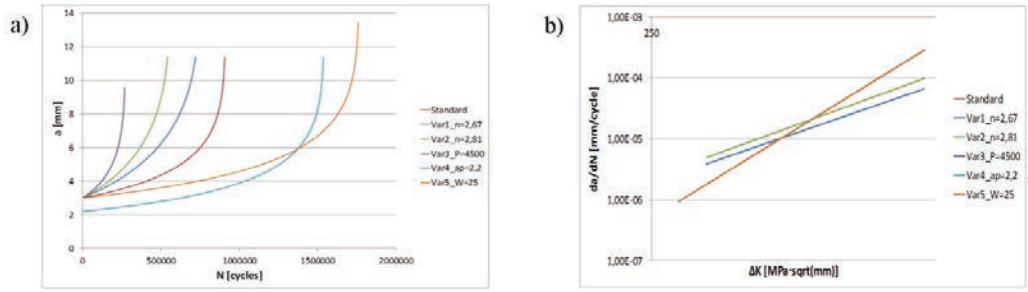

Fig. 9. (a) *a*-*N*-plot in linear representation; (b) *da/dN*-ΔK-plot in log-log-representation.

In figure 10a) an *a*-*ΔK*-plot in linear scale can be seen. The graphs with the largest and smallest crack lengths can be matched with the largest probe height and the largest force. The other calculations don't differ much in their graphs. This leads to the conclusion, that the variables in the first factor of formula (3) play a leading role in the calculation of crack lengths. For the load *P* this conclusion is easily made. For the probe height *W* further investigations will be needed, as also the geometry function *g* from formula (3) depends on *W* and thus plays its role in the calculation.

Figure 10b) shows a *N*-*ΔK*-plot. It can be seen, that the same stress intensity factor at the crack tip can be reached after very different lifetimes of the crack. Here also the before mentioned tendencies can be seen. The Variation of *C* and *n* seems to play a smaller role in the calculation of the service life of a probe than the variation of the geometry of the probe or the loads.

It can be seen from the calculations that an increase of the load of about 20% leads to a reduction of the service life of a probe on a third. A reduction of the length of a_p from 3 mm to 2.2 mm (27%) leads to a five times longer service life.

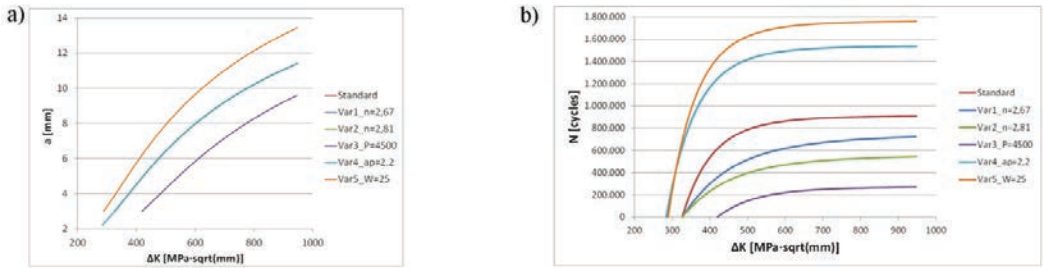

Fig. 10. (a) *a*-*ΔK*-plot in linear representation; (b) *N*-*ΔK*-plot in linear representation.

6. Outlook

In the future course of the project, real experiments with different load levels, R-Ratios and temperatures will be carried out. The results obtained there shall be compared with the calculations presented in this paper. This will show how reliable predictions made with the crack growth formulae are.

In order to optimize the service life calculations of real rails, numeric indicators for the importance of certain parameters will be searched for. As stated before, the applied load or the detectable length of a starting crack may be such parameters. These findings have to be verified with the crack growth formulae that fit for the cracks in the rail foot.

Acknowledgements

The work presented is carried out as part of a joint research project (2014–2016). This project P1033 of the research association (FOSTA) was financed over the AiF within the development program for industrial community research and development (IGF-Nr. 18094N) from the Federal Ministry of Economic Affairs and Energy (BMWi) based on a decision of the German Bundestag. The authors thank all partners for their cooperation. Also to the supporting companies special thanks are given.

References

BSI ISO 12108:2012. Metallic materials – Fatigue testing – Fatigue crack growth method. BSI Standards Limited 2012.

Deutsche Bundesbahn, BZA München, Dez. 85A: Dauerfestigkeitsschaubild nach Smith für UIC 60 (900), 1989 (not published).

Deutscher Stahlbau-Verband, 1996. Stahlbau Handbuch. Stahlbau-Verlagsgesellschaft mbH. Köln. 1996.

DIN EN 1991-2:2010. Eurocode 1: Einwirkungen auf Tragwerke – Teil 2: Verkehrslasten auf Brücken; Deutsche Fassung EN 1991--2:2003+AC:2010. DIN – Deutsches Institut für Normung. Dezember 2010.

Edel, K.-O., 2015. Einführung in die bruchmechanische Schadensbeurteilung. Wiesbaden: Springer Vieweg.

Freystein, H., 2012. Untersuchungen zu den zulässigen zusätzlichen Schienenspannungen aus Interaktion Gleis/Brücke. Dissertation. Technische Universität Berlin. 2012.

Haibach, E., 2006. Betriebsfestigkeit : Verfahren und Daten zur Bauteilberechnung. Berlin, Heidelberg, New York: Springer. 3. Korrigierte und ergänzte Auflage. 2006.

Kopp, E., 1970. Ein Beitrag zur Ermittlung der zulässigen Liegedauer von Eisenbahnschienen. Mitteilung des Instituts für Bau von Landverkehrswegen der Technischen Universität München, Heft 14. 1970.

Romano, S., Manenti, D., Beretta, S., Zerbst, U., 2015. Probabilistic method for residual lifetime and inspection interval of aluminothermic welded rails with foot cracks (not published)

Ruge, P., Birk, C., Muncke, M., Schmälzlin, G., 2005. Schienenlängskräfte auf Brücken bei nichtlinearer Überlagerung der Lastfälle Temperatur, Tragwerksbiegung, Bremsen. Bautechnik 82 (2005), Heft 11. Ernst&Sohn, Berlin.

Schramm, N., 2014. Beitrag zur wirklichkeitsnahen Ermittlung von Schienenspannungen im Übergangsbereich zu Brückentragwerken. Technische Universität München, Lehrstuhl für Massivbau. Master's Thesis. 2014.

Schnitzer, T., Edel, K.-O., Bohne, I., 2004. Fahrflächenschäden. Fachhochschule Brandenburg. 2004.

Tóth, L., Romvari, P., 1980/81. Sinacélok törésmechanikai anyagjellemzöi (fracture mechanical parameters of rail steels). Technical University of Heavy Industry, Chair for mechanical technology, Miskolc. 1980/1981.